Multi-fingered Telemanipulation - Mapping of a Human Hand to a Three Finger Gripper

Angelika Peer, Stephan Einenkel, and Martin Buss

***Abstract*— If a teleoperation scenario foresees complex and fine manipulation tasks a multi-fingered telemanipulation system is required. In this paper a multi-fingered telemanipulation system is presented, whereby the human hand controls a three-finger robotic gripper and force feedback is provided by using an exoskeleton. Since the human hand and robotic grippers have different kinematic structures, appropriate mappings for forces and positions are applied. A point-to-point position mapping algorithm as well as a simple force mapping algorithm are presented and evaluated in a real experimental setup.**

I. Introduction

In a teleoperation scenario tasks are performed by a mechanical manipulator controlled remotely by a human operator provided with a force reflecting haptic interface, which enables the interaction with the remote environment. If dextrous telemanipulation tasks are required, the telemanipulator is additionally equipped with robotic grippers or robot hands, which must be controlled by the human operator.

Thus, in a multi-fingered telemanipulation system a kinematic mapping between human and robot hand motions is necessary. Commonly the following three mapping methods can be distinguished: joint-to-joint mapping, pose mapping, and point-to-point mapping.

The joint-to-joint mapping (or joint angle mapping) is typically applied to telemanipulation systems with an anthropomorphic robot hand [1]. The similarity between human and robot hand kinematics allows to simply map the finger joint angles without any further transformation. In some works the similarity of human and robot hand motion is further achieved by restricting the human finger motions with an exoskeleton [2]. The joint-to-joint mapping is especially suitable for enveloping and power grasps. Unfortunately, many of the existing robot hands are not of anthropomorphic type and thus this method is not applicable.

The pose mapping tries to find robot hand poses, which can be correlated to human hand poses. In [3] a corresponding transformation matrix with human finger angles as input and robot joint angles as output has been derived; an interpolation algorithm is used when switching between the single poses. Recently also grasp identification methods based on neural networks have been developed [4]. Dependent on the identified grasp, different types of predefined joint-to-joint mappings (which represent a special pose) are applied. [5] uses hidden markov models to identify the grasp type and a neural network to choose between predefined joint angle mappings.

Some sorts of pose mapping can also be found in the field of "programming-by-demonstration". In [6] a nearest neighbor grasp recognition algorithm based on the analysis of the measured finger joint angles is presented. A joint-to-joint mapping is applied to generate different grasp patterns, which are stored in a library and carried out if the corresponding grasp type is identified. In [7] firstly the grasp type is identified, then a correct grasp pose is chosen and a force-controlled grasping by closing the fingers is applied. In [8] finally a mapping method based on a virtual finger is presented.

When applying one of the presented pose mappings for a telemanipulation system, the reliability and stability of the grasp identification process plays an important role. This is the case since in a telemanipulation scenario continuous identification of the human grasp type is necessary. A well known problem of the pose mapping is namely the unpredictable switching of the robot hand between different kind of grasp types, when small changes of the human hand posture occur. On this account only simple grasp postures can be realized and hence the method is applied in a limited way in telemanipulation systems.

The most common approach used for mapping of human to robot hand postures is the point-to-point or fingertip mapping, whereby the fingertip positions of the human hand are mapped to the robot fingertip positions [9]–[11]. In order to apply such an approach the computation of the forward kinematics of the human hand, the mapping of the fingertip positions, and finally the determination of the robot joint angles by applying the corresponding inverse kinematics are required. Such a mapping algorithm is appropriate to represent fingertip positions and is therefore commonly applied for precision grasps.

In this paper a point-to-point mapping algorithm for a multi-fingered telemanipulation system is presented, which allows to map fingertip motions of the human hand to a three-finger robotic gripper, the BarrettHand. Existing mapping algorithms for this gripper, see [5], [7], [12], allow only semi-autonomous teleoperation, whereby prior knowledge about the user's intention and the object to be manipulated is used to select an appropriate grasp type, which is then executed autonomously. The reliability of these mapping algorithms depend strongly on the identification process of objects and the estimation of human's intention. By contrast, the here presented mapping algorithm does not require any knowledge about size and form of objects or human's intention. This

A. Peer, S. Einenkel and M. Buss are with the Institute of Automatic Control Engineering, Technische Universität München, Germany. angelika.peer@tum.de, einenkel@gmx.net, mb@tum.de

makes it more reliable as well as easier to understand and to predict. Moreover, no library with predefined grasp types is necessary.

II. Description of Telemanipulation System

In order to perform complex manipulation tasks a multi-fingered telemanipulation system consisting of a three-finger robotic gripper (BarrettHand), a dataglove (CyberGlove) and an exoskeleton (CyberGrasp) has been developed. The usage of a universal gripper allows to operate in highly variable, unstructured, unknown or dynamic working environments. As a part of a telemanipulation system the gripper is controlled by a human operator. On this account human hand and finger motions are measured using a data glove system and then mapped to the gripper. Sensed interaction forces are fed back to the operator and displayed through a haptic display, an exoskeleton. Since human hand and gripper have different kinematic structures, appropriate mappings for forces and motion between the finger and the gripper are required. Fig. 1 shows the resulting system architecture. Below their components are presented in detail.

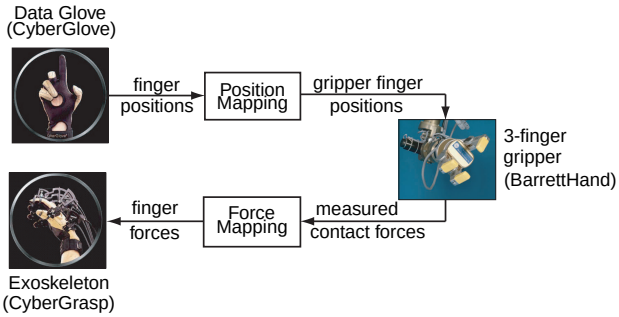

Fig. 1. System architecture of the multi-fingered telemanipulation system

1) Grippers: A *BarrettHand* (BH) from Barrett Technology Inc. is used as gripper, see [13]. The *BarrettHand* has three fingers with four actuated degrees of freedom. Each finger consists of two coupled joints driven by a single DC brushless servo motor. In addition, two fingers can rotate synchronously and symmetrically arround the base joint in a spreading action. Each finger is equipped with a strain gage joint torque sensor, for measuring the torque externally applied about the distal joint over a range of +/-1 Nm. Real time operation of the motors is assured by a low level velocity controller. The high level controllers, as e.g. position control, are realized on the PC using MATLAB/Simulink Real-Time Workshop and RTAI Linux.

2) Data Glove System: To capture finger and hand motions the data glove system *CyberGlove* from Immersion Corporation, see [14], is used. The data glove is equipped with 22 sensors located over or near the joints of the hand and the wrist. A resistive bend-sensing technology is used to transform hand and finger motions into real-time digital joint-angle data. In order to map human hand to robot hand motions, an appropriate position mapping has to be implemented.

3) Exoskeleton: In order to provide force feedback to the human operator the *CyberGrasp* system, an exoskeleton from Immersion Corporation, see [15], is used. The exoskeleton is attached to the back of the human hand and guides force-applying tendons to the user's fingertips. Desired force values are sent to the local force controller provided by the manufacturer. Since each finger is only equipped with one tendon only pull but no push-forces can be applied. Similar to the position mapping algorithm, also a force mapping algorithm is necessary. In the following these algorithms are described in more detail.

III. Position Mapping

For the mapping of the human to robot hand motions, a point-to-point position mapping has been applied. The principle of the implemented algorithm is shown in Fig. 2. The already presented data glove system is used to measure the human finger joint angles. These angles, in combination with some prior knowledge about the human hand kinematics, are used to compute the fingertip positions of the human hand (FK). These fingertip positions again are mapped to fingertip positions of the robotic gripper. Finally, the motor joint angles of the BarrettHand are determined by using the corresponding inverse kinematics (IK). A detailed description of each component is given in the following.

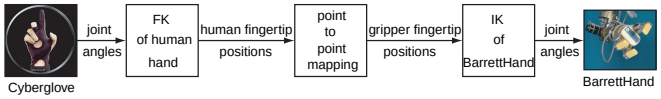

Fig. 2. Scheme of position mapping

A. Kinematics of human hand

Fig. 3 shows the human hand kinematics. A finger composes of a distal $l_{k,d}$, proximal $l_{k,p}$ and metacarpal $l_{k,m}$ link connected by the corresponding joint angles $q_{k,d}$, $q_{k,p}$, $q_{k,m}$ with $k = 1, \ldots, 5$. The abduction is described by the joint angle $q_{k,a}$. According to this kinematic model the fingertip positions with respect to the hand coordinate system can be calculated as follows:

$$^{H}\boldsymbol{x}_k\left(\boldsymbol{q}_k\right) = \boldsymbol{a}_k\left(\boldsymbol{q}_k\right) + \boldsymbol{r}_k \quad \text{with } k = 1 \ldots 5, \qquad (1)$$

whereby $\boldsymbol{q}_k = \left[q_{k,d},\ q_{k,p},\ q_{k,m},\ q_{k,a}\right]^T$ denotes the joint angles of the k-th finger and $\boldsymbol{r}_k$ is a translation vector. The vectors $\boldsymbol{a}_k\left(\boldsymbol{q}_k\right)$ are defined as follows:

$$\boldsymbol{a}_k = \begin{bmatrix} \sin q_{k,a}\left(l_{k,m}\cos q_{k,m} + l_{k,p}\cos(q_{k,m}+q_{k,p})+\right. \\ \cos q_{k,a}\left(l_{k,m}\cos q_{k,m} + l_{k,p}\cos(q_{k,m}+q_{k,p})+\right. \\ l_{k,m}\sin q_{k,m} + l_{k,p}\sin(q_{k,m}+q_{k,p})+ \\ l_{k,d}\cos(q_{k,m}+q_{k,p}+q_{k,d})\big) \\ l_{k,d}\cos(q_{k,m}+q_{k,p}+q_{k,d})\big) \\ l_{k,d}\sin(q_{k,m}+q_{k,p}+q_{k,d}) \end{bmatrix}$$

for the index, middle, ring finger and pinkie ($k = 2, \ldots, 5$) and

$$\boldsymbol{a}_1 = \begin{bmatrix} l_{1,d}\left(-\sin q_{1,m}\sin(q_{1,p}+q_{1,d}) + \cos q_{1,m}\cos\hat{q}_{1,a}\cos(q_{1,p}+q_{1,d})\right) + \\ -\sin\hat{q}_{1,a}\left(l_{1,m} + l_{1,p}\cos q_{1,p} + l_{1,d}\cos(q_{1,p}+q_{1,d})\right) + \\ -l_{1,d}\left(\sin q_{1,m}\cos\hat{q}_{1,a}\cos(q_{1,p}+q_{1,d}) + \cos q_{1,m}\sin(q_{1,p}+q_{1,d})\right) + \\ l_{1,p}\left(\cos q_{1,m}\cos\hat{q}_{1,a}\cos q_{1,p} - \sin q_{1,m}\sin q_{1,p}\right) + l_{1,m}\cos q_{1,m}\cos\hat{q}_{1,a} \\ 0 \\ -l_{1,p}\left(\sin q_{1,m}\cos\hat{q}_{1,a}\cos q_{1,p} + \cos q_{1,m}\sin q_{1,p}\right) - l_{1,m}\sin q_{1,m}\cos\hat{q}_{1,a} \end{bmatrix}$$

for the thumb ($k = 1$), whereby $\hat{q}_{1,a} = q_{1,a} + q^o_{1,a}$ with $q^o_{1,a}$ a joint angle offset.

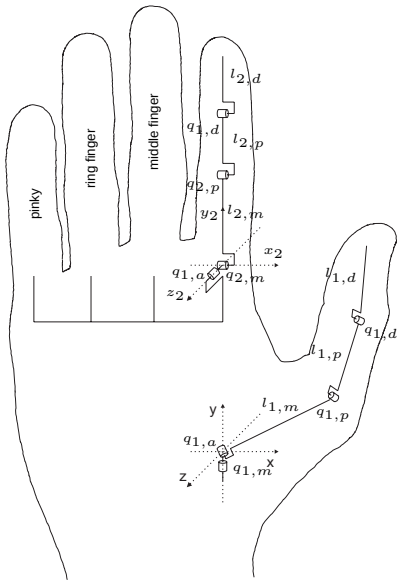

Fig. 3. Kinematic model of the right human hand

B. BarrettHand kinematics

In this subsection some details about the BarrettHand kinematics are given, whereby all technical figures are taken from [16].

The BarrettHand is a gripper with three identical fingers. While the finger F3 is fixed to the carpus, the fingers F1 and F2 are able to rotate $180°$ around the base. Each finger consists of three links with the lenghts l_1, l_2, l_3 and two joints with the joint angles $q_{Fk,2}$ and $q_{Fk,3}$, whereby the index Fk stands for the k-th finger. Fig. 4 shows a side view of the BarrettHand with all mentioned parameters. The fingers F1 and F3 are completely opened and finger F2 is flexed. The spread angle $q_{Fk,1}$ is shown in Fig. 5.

Since the BarrettHand fingers cannot be stretched completely, the joint angle $q_{Fk,2}$ is composed of a variable $\Theta_{Fk,2}$ and a constant part $\Phi_2 = 2.46°$

$$q_{Fk,2} = \Theta_{Fk,2} + \Phi_2 \quad \text{with} \quad 0° \leq \Theta_{Fk,2} \leq 140°. \tag{2}$$

Similarly the joint angle $q_{Fk,3}$ is given by

$$q_{Fk,3} = \Theta_{Fk,3} + \Phi_3 \quad \text{with} \quad 0° \leq \Theta_{Fk,3} \leq 48°,\ \Phi_3 = 50° \ . \tag{3}$$

The BarrettHand disposes of four actuators, one per finger plus one for the abduction. The relation between the four motor joints Θ_{M1} to Θ_{M4} and the variable part $\Theta_{Fk,i}$ of the joint angles $q_{Fk,i}$ is described by the following equation:

$$\begin{bmatrix} \Theta_{F1,1} \\ \Theta_{F1,2} \\ \Theta_{F1,3} \\ \Theta_{F2,1} \\ \Theta_{F2,2} \\ \Theta_{F2,3} \\ \Theta_{F3,2} \\ \Theta_{F3,3} \end{bmatrix} = \begin{bmatrix} 0 & 0 & 0 & -2/35 \\ 1/125 & 0 & 0 & 0 \\ 1/375 & 0 & 0 & 0 \\ 0 & 0 & 0 & 2/35 \\ 0 & 1/125 & 0 & 0 \\ 0 & 1/375 & 0 & 0 \\ 0 & 0 & 1/125 & 0 \\ 0 & 0 & 1/375 & 0 \end{bmatrix} \cdot \begin{bmatrix} \Theta_{M1} \\ \Theta_{M2} \\ \Theta_{M3} \\ \Theta_{M4} \end{bmatrix} . \tag{4}$$

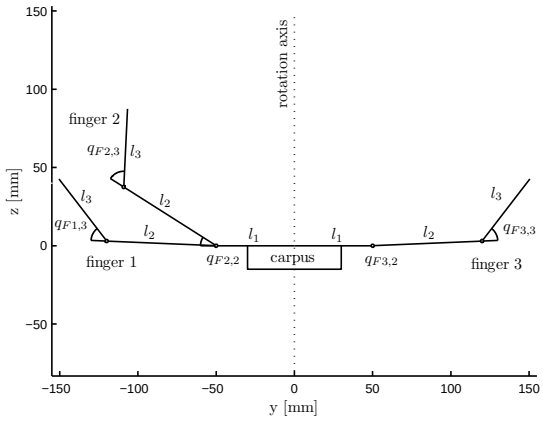

Fig. 4. Side view of the BarrettHand

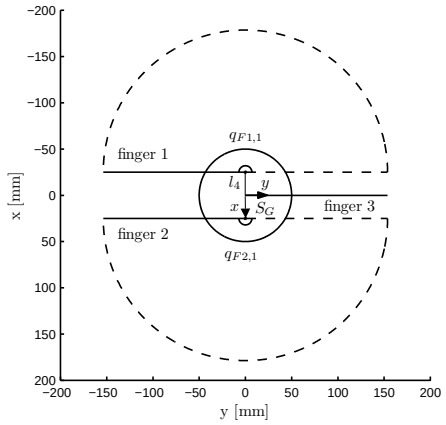

Fig. 5. Top view of the BarrettHand

As can be seen from these equations, the two spread angles $q_{F1,1}$ and $q_{F2,1}$ are coupled and thus the following relationship holds:

$$q_{F1,1} = \Theta_{F1,1} = -\Theta_{F2,1} = -q_{F2,1} \ . \tag{5}$$

Also the joint angles $q_{Fk,2}$ and $q_{Fk,3}$ are coupled:

$$\Theta_{Fk,2} = 3\Theta_{Fk,3} \ , \tag{6}$$

$$q_{Fk,2} - \Phi_2 = 3(q_{Fk,3} - \Phi_3) \ . \tag{7}$$

These couplings have severe consequences, since the fingertips cannot be positioned in an arbitrary manner but can be moved only along a certain trajectory. This trajectory is shown in Fig. 6.

1) Forward kinematics: The forward kinematics of the BarrettHand describes the Cartesian fingertip position ${}^G\boldsymbol{x}_k$ in the gripper coordinate system S_G as a function of the motor angles Θ_{M1} to Θ_{M4}. The fingertip position in the corresponding finger coordinate system S_F (see Fig. 6) is given by:

$${}^F\boldsymbol{x}_{Fk} = \begin{bmatrix} 0 \\ l_1 + l_2 \cos q_{Fk,2} + l_3 \cos(q_{Fk,2} + q_{Fk,3}) \\ l_2 \sin q_{Fk,2} + l_3 \sin(q_{Fk,2} + q_{Fk,3}) \end{bmatrix} . \tag{8}$$

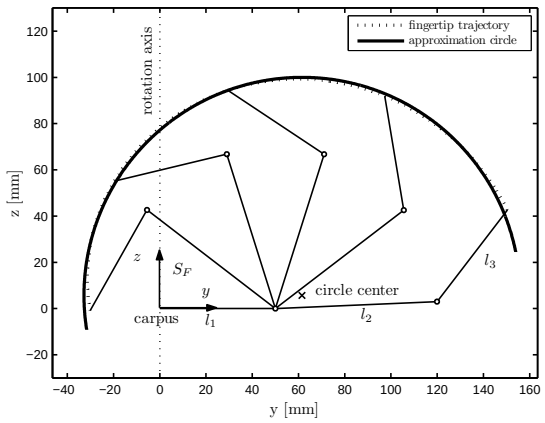

Fig. 6. Trajectory of the gripper fingertips in the finger coordinate system

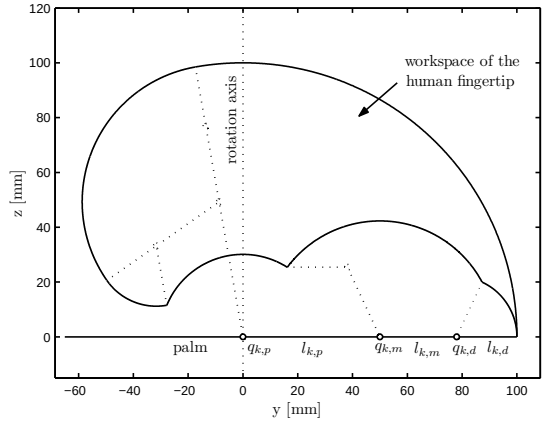

Fig. 7. Workspace of a typical human finger in y-z-plane with the link lengths l_m =50mm, l_p =28mm, l_d =22mm

To compute the Cartesian position in the gripper coordinate system, ${}^F\boldsymbol{x}_{Fk}$ must be multiplied by a rotation matrix $\boldsymbol{R}$ and displaced by a translation vector $\boldsymbol{t}$:

$$ {}^G\boldsymbol{x}_{Fk} = \boldsymbol{R}(\boldsymbol{\gamma}) {}^F\boldsymbol{x}_{Fk} + \boldsymbol{t} \ , \tag{9} $$

whereby

$$ \boldsymbol{R}(\gamma) = \begin{bmatrix} \cos(\gamma) & \sin(\gamma) & 0 \\ -\sin(\gamma) & \cos(\gamma) & 0 \\ 0 & 0 & 1 \end{bmatrix}, \ \gamma \in \{q_{F1,1}, -q_{F2,1}, \pi\} $$

and

$$ \boldsymbol{t} = \begin{bmatrix} \ jl_4, 0, 0 \ \end{bmatrix}^T, \quad j \in \{-1, 1, 0\} $$

for the corresponding finger $\{F1, F2, F3\}$.

2) Inverse kinematics: For the BarrettHand an analytical inverse kinematics can be computed: In a first step the spread angle $q_{Fk,1}$ has to be determined. In order to do so the fingertip positions given in the gripper coordinate system S_G are transformed into an equal oriented coordinate system $S_{G'}$ with origin in the finger base point:

$$ {}^{G'}\boldsymbol{x}_{Fk} = {}^G\boldsymbol{x}_{Fk} - \boldsymbol{t} \ . \tag{10} $$

Given the fingertip position of F1 in this transformed coordinate system ${}^{G'}\boldsymbol{x}_{F1} = [x_1', y_1', z_1']$, the joint angle $q_{F1,1}$ can be easily worked out:

$$ q_{F1,1} = -\arctan \frac{x_1'}{y_1'} \ . \tag{11} $$

The motor angle Θ_{M4} can then be calculated by using (4) and (5).

Using the spread angle $q_{Fk,1}$, the Cartesian position in the finger coordinate system S_F can be computed by solving (9) for ${}^F\boldsymbol{x}_{Fk}$. Inserting these fingertip positions into

$$ q_{Fk,3} = \arccos\left(\frac{(y_{Fk} - l_1)^2 + z_{Fk}^2 - l_2^2 - l_3^2}{2 l_2 l_3} \right) \ , \tag{12} $$

$$ q_{Fk,2} = \arccos\left(\frac{z_{Fk}\,(l_3 \sin q_{Fk,3})}{(l_2 + l_3 \cos q_{Fk,3})^2 + l_3^2 \sin^2 q_{Fk,3}} + \frac{(y_{Fk} - l_1)\,(l_2 + l_3 \cos q_{Fk,3})}{(l_2 + l_3 \cos q_{Fk,3})^2 + l_3^2 \sin^2 q_{Fk,3}} \right) \tag{13} $$

the corresponding joint angles result. (12) and (13) are hereby determined when solving (8) for $q_{Fk,2}$ and $q_{Fk,3}$. Finally considering (2), (3) and (4) the motor joint angle Θ_{Mk} is given by

$$ \Theta_{Mk} = 125\,(q_{Fk,2} - \Phi_2)\,\frac{180}{\pi} \ , \quad \text{or} \tag{14} $$

$$ \Theta_{Mk} = 375\,(q_{Fk,3} - \Phi_3)\,\frac{180}{\pi} \ . \tag{15} $$

If two different solutions are obtained, the desired position is not reachable with the BarrettHand.

C. Point-to-point mapping by vertical projection

Fig. 7 shows the workspace of a typical human finger. Since hyperextension is not important when grasping an object, for this drawing the minimal joint angles have been set to zero. The maximal considered joint angles have been taken from [17] and are reported in Table I.

TABLE I
MINIMAL AND MAXIMAL JOINT ANGLES OF A HUMAN FINGER

joint angles	q_m	q_p	q_d
minimal	0	0	0
maximal	100	115	65

Comparing the workspace of a human finger with that of a BarrettHand finger (as shown in Fig. 6) one can see that the human fingertip position has to be projected onto a trajectory feasible with the BarrettHand. The drawback of this method is obvious: different positions of the human fingertip are mapped onto the same fingertip position of the robotic gripper. This is the case because of the prior presented couplings of the BarrettHand joint angles. A possible projection method is presented in the following paragraphs:

In the first step, each BarrettHand finger must be assigned to a human finger. Since F3 of the BarrettHand is opposed to F1 and F2, this finger is mapped to the thumb. Considering the right hand, F1 is used to map the index finger. For F2 either middle finger, ring finger or pinky can be selected. Since the pinky does not play an important role in manipulations, typically the middle or ring finger is mapped. As

the range of abduction of the BarrettHand is quite huge, the ring finger is selected.

The proposed position mapping algorithm adapts the workspace of the human fingers to the workspace of the BarrettHand by using a scaling factor. For simplicity a simple scalar scaling factor g_p is used. Then the workspace of the human fingers is vertically projected onto the trajectory of the BarrettHand. Fig. 8 shows the workspace of the human finger, the workspace of the BarrettHand, as well as the projection principle. For the sake of clarity, the workspace of the human finger is drawn above the BarrettHand trajectory.

Aligning the rotation axis of the human index finger and one of the BarrettHand fingers, the abduction angle to be set for the gripper can be easily determined from the abduction angles of the human hand. Given the abduction between index and middle finger $q_{2,a}$ and between middle and ring finger $q_{3,a}$, the abduction angle for the BarrettHand is defined as follows

$$q_{F1,1} = -q_{F2,1} = \frac{1}{2}\left(q_{2,a} + q_{3,a}\right) \quad . \tag{16}$$

The factor 1/2 results from the fact that the angle between F1 and F2 of the BarrettHand is given by $2q_{Fk,1}$.

The adaptation of the human hand workspace to the BarrettHand workspace is realized by a scaling factor g_p. Hereby, the ratio of maximally opened human and BarrettHand finger is used. For the index and ring finger the scaling factor is given by

$$g_{p_k} = \frac{l_1 + l_2\cos\Phi_2 + l_3\cos\left(\Phi_2 + \Phi_3\right)}{\left(l_{k,m} + l_{k,p} + l_{k,d}\right)} \quad \text{for} \quad k = 1, 2 \tag{17}$$

and for the thumb by

$$g_{p_3} = \frac{l_1 + l_2\cos\Phi_2 + l_3\cos\left(\Phi_2 + \Phi_3\right)}{l_t} \quad . \tag{18}$$

To finally project the finger position on the BarrettHand trajectory the motor angles for a given y-coordinate of the scaled human hand position have to be computed. Since the inverse kinematics given by (12) and (13) requires the knowledge of the y and z-coordinate of the BarrettHand finger, the corresponding z-coordinate has to be determined first. As without knowledge of the single joint angles it is not possible to compute the z-coordinate of the BarrettHand finger if the y-coordinate is given, the trajectory of the BarrettHand is approximated by a circle as shown in Fig. 6. Except for the two extreme positions, the error introduced by this approximation is less then one millimeter. Other approximation methods as splines might be able to better fit the fingertip trajectory, but do not provide any benefit taking into account the human ability for fingertip position perception. In the first step the finger position is projected on the approximation circle and then the motor joint angle is computed by using the exact inverse kinematics given by (13) and (14) or (12) and (15).

IV. Force mapping

Each finger of the BarrettHand is equipped with a strain gage joint torque sensor, which allows measuring the torque

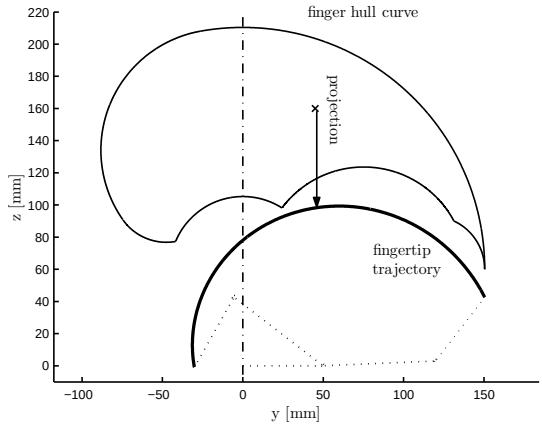

Fig. 8. Vertical projection of fingertip position on BarrettHand trajectory

applied on the distal joint. On this account, normal forces F_k applied to the fingertip can be determined as follows:

$$f_k = \frac{\tau_k}{l_3} \quad \text{for} \quad k = 1, \ldots, 3 \ , \tag{19}$$

whereby τ_k is the measured torque and l_3 the corresponding moment arm. These forces are fed back to the master site and displayed by the exoskeleton. To guarantee stability of the overall teleoperation system the forces are multiplied by a scaling factor g_f, which has to be selected appropriately.

V. Experimental evaluation

The above presented mapping algorithms for position and force have been implemented in the real hardware setup, whereby the single components are connected as already depicted in Fig. 1. Some of the obtained results are further discussed in succeeding paragraphs.

Using the position mapping algorithm, described in Sec. III distances between the fingertips and the corresponding finger coordinate system are mapped with a scaling factor g_p onto the BarrettHand. One of the advantages of this position mapping is that the principle form of the grasp type is hereby maintained, which makes it easy to predict the gripper motion and thus simplifies the execution of the telemanipulation task. Fig. 9 shows some examples of different poses of the human hand and the corresponding pose of the BarrettHand. For the sake of clearity the pictures have been made without wearing the CyberGrasp. As can be seen, different grasp, as defined by [18], namely precision and power grasps, can be performed. Thus, the mapping is suitable for a variety of different manipulation tasks.

One drawback of this position mapping method is that the workspace of the human hand is not completely covered by the BarrettHand. As can be seen from Fig. 8, finger positions with small y-values cannot be mapped. As such finger configurations are only rarely used in manipulation tasks this effect is of minor importance. Nonetheless, it should be mentioned that there exist also other possibilities to project the human finger position onto the BarrettHand trajectory. A further possibility, not reported here, is presented in [19], which tries to better fit the workspace of human and BarrettHand fingers.

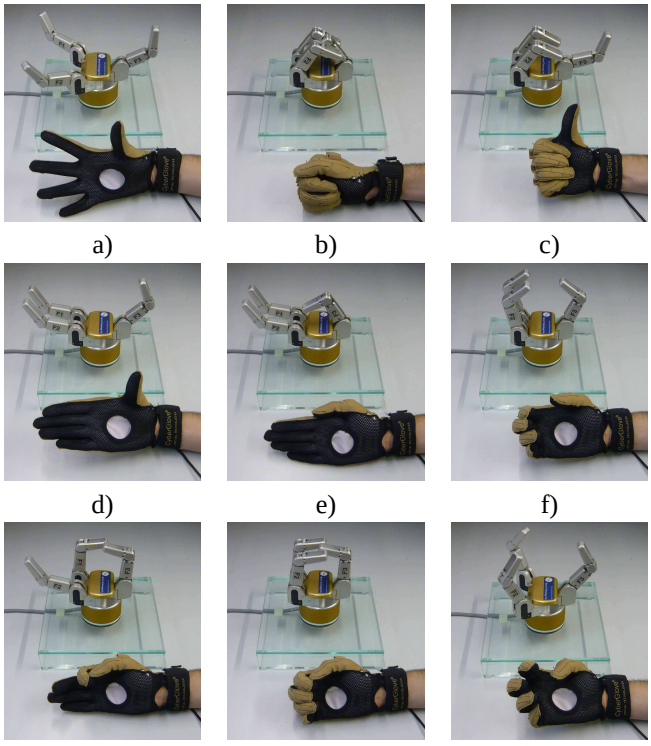

Fig. 9. Human hand and corresponding BarrettHand poses

Evaluations of the proposed force mapping algorithm indicate that people can clearly distinguish between a soft and a strong grasp. The limited range of the BarrettHand torque sensor however, restricts the range of applicable forces significantly. A further difficulty observed here is that the BarrettHand uses torque and not force sensors. If humans touch objects vertically with one of the fingertips no interaction forces can be detected as the moment arm is zero. This has to be taken into account if interacting with objects. Finally, it should be mentioned that the quite huge friction in the tendons of the CyberGrasp makes it difficult to apply really small forces. This can be explained by stick-slip effects that occur in the tendons.

Nonetheless it can be stated that the implemented position and force mapping algorithms allow to interact in a very intuitive way with the remote environment, despite of a non-anthropomorphic kinematics of the grippers and a relative poor force feedback performance.

VI. Summary and Conclusion

A multi-fingered telemanipulation system has been presented, whereby a human operator controls a three-finger robotic gripper and force-feedback is provided by using an exoskeleton. The different kinematic structure of human and robot hand required the implementation of appropriate force and position mappings. After reviewing typical approaches for the mapping of a human to a robotic hand a point-to-point position mapping algorithm has been presented. On this account forward kinematics of the human hand and inverse kinematics of the BarrettHand were derived and a position mapping algorithm based on a projection of the human fingertip position on the gripper trajectory has been proposed. The evaluation in first real hardware experiment showed a good performance of the position mapping as a variety of different grasp types ranging from precision to power grasps can be performed. The quality of the force feedback is strongly affected by the maximum torque measurable by the BarrettHand and the performance of the force controller. Further evaluations of the implemented algorithms, e.g. in form of psychophysical experiments are subject of future research.

References

[1] K. Kyriakopoulos, J. Van Riper, A. Zink, and H. Stephanou, "Kinematic Analysis and Position/Force Control of the Anthrobot Dextrous Hand," *IEEE Trans. on Systems, Man and Cybernetics*, vol. 27, no. 1, pp. 95–104, February 1997.

[2] A. Wright and M. Stanisic, "Kinematic Mapping between the EXOS Handmaster Exoskeleton and the Utah-MIT Dextrous Hand," in *Proc. of the IEEE International Conference on Systems Engineering*, 1990, pp. 809–811.

[3] L. Pao and T. Speeter, "Transformation of Human Hand Positions for Robotic Hand Control," in *Proc. of the IEEE International Conference on Robotics and Automation*, vol. 3, May 1989, pp. 1758–1763.

[4] T. Wojtara and K. Nonami, "Hand Posture Detection by Neural Network and Grasp Mapping for a Master Slave Hand System," in *Proc. of the IEEE/RSJ International Conference on Intelligent Robots and Systems*, vol. 1, Sept., Oct. 2004, pp. 866–871.

[5] S. Ekvall and D. Kragic, "Interactive Grasp Learning Based on Human Demonstration," in *Proc. of the IEEE International Conference on Robotics and Automation*, vol. 4, April, May 2004, pp. 3519–3524.

[6] J. Aleotti and S. Caselli, "Grasp Recognition in Virtual Reality for Robot Pregrasp Planning by Demonstration," in *Proc. of IEEE International Conference on Robotics and Automation*, May 15-19, 2006, pp. 2801–2806.

[7] M. Ehrenmann, R. Zollner, O. Rogalla, and R. Dillmann, "Programming Service Tasks in Household Environments by Human Demonstration," in *Proc. of the 11th IEEE International Workshop on Robot and Human Interactive Communication*, September 2002, pp. 460–467.

[8] S. Kang and K. Ikeuchi, "Toward Automatic Robot Instruction from Perception-Mapping Human Grasps to Manipulator Grasps," *IEEE Trans. on Robotics and Automation*, vol. 13, no. 1, pp. 81–95, February 1997.

[9] R. Rohling and J. Hollerbach, "Optimized Fingertip Mapping for Teleoperation of Dextrous Robot Hands," in *Proc. of the IEEE International Conference on Robotics and Automation*, vol. 3, May 1993, pp. 769–775.

[10] M. Fischer, P. van der Smagt, and G. Hirzinger, "Learning Techniques in a Dataglove Based Telemanipulation System for the DLR Hand," in *Proc. of the IEEE International Conference on Robotics and Automation*, vol. 2, May 1998, pp. 1603–1608.

[11] J. Hong and X. Tan, "Calibrating a VPL DataGlove for Teleoperating the Utah/MIT Hand," in *Proc. of the IEEE International Conference on Robotics and Automation*, vol. 3, May 1989, pp. 1752–1757.

[12] S. Berman, J. Friedman, and T. Flash, "Object-action Abstraction for Teleoperation," in *Proc. of the IEEE International Conference on Systems, Man and Cybernetics*, vol. 3, October 2005, pp. 2631–2636.

[13] Barrett Technology Inc , "BarrettHand," http://www.barrett.com/robot/products-hand.htm, April 2008.

[14] Immersion Corp , "CyberGlove II Wireless Data Glove," http://www.immersion.com/3d/products/cyber_glove.php, April 2008.

[15] ——, " CyberGrasp Exoskeleton," http://www.immersion.com/3d/products/cyber_grasp.php, April 2008.

[16] *BarrettHand BH8-Series User Manual, Firmware Version 4.3x*, Barrett Technology Inc., February 2002.

[17] C. Droste and M. von Planta, *Memorix, Edition Medizin*, 2nd ed. Weinheim: Wiley-VCH, 1989.

[18] M. Cutkosky, "On Grasp Choice, Grasp Models, and the Design of Hands for Manufacturing Tasks," *IEEE Trans. on Robotics and Automation*, vol. 5, no. 3, pp. 269–279, June 1989.

[19] S. Einenkel, "Kalibrierung und Abbildung der menschlichen Hand auf einen dreifingrigen Greifer zur mehrfingrigen Telemanipulation," Master's thesis, Technische Universität München, 2006, *in german*.